

# Elemental Analysis of Freeze-dried Thin Sections of *Samanea* Motor Organs: Barriers to Ion Diffusion through the Apoplast

RUTH L. SATTER, ROBERT C. GARBER, LAMIA KHAIRALLAH, and YI-SHAN CHENG  
*Biological Sciences Group, U-42, University of Connecticut, Storrs, Connecticut 06268; and Department of Plant Pathology, Cornell University, Ithaca, New York 14853*

**ABSTRACT** Leaflet movements in the legume *Samanea saman* are dependent upon massive redistribution of potassium (K), chloride (Cl), and other solutes between opposing (extensor and flexor) halves of the motor organ (pulvinus). Solute diffusion is known to occur through the apoplast during redistribution. To test the possibility that solute diffusion might be restricted by apoplastic barriers, we analyzed elements in the apoplast in freeze-dried cryosections of pulvini using scanning electron microscopy/x-ray microanalysis. Large discontinuities in apoplastic K and Cl at the extensor-flexor interface provide evidence for a barrier to solute diffusion. The barrier extends from the epidermis on upper and lower sides of the pulvinus to cambial cells in the central vascular core. It is completed by hydrophobic regions between phloem and cambium, and between xylem rays and surrounding vascular tissue, as deduced by discontinuities in apoplastic solutes and by staining of fresh sections with lipid-soluble Sudan dyes. Thus, symplastic pathways are necessary for ion redistribution in the *Samanea* pulvinus during leaflet movement.

In pulvini from leaflets in the closed state, all cells on the flexor side of the barrier have high internal as well as external K and Cl, whereas cells on the extensor side have barely detectable internal or external K or Cl. Approximately 60% of these ions are known to migrate to the extensor during opening; all return to the flexor during subsequent closure. We propose that solutes lost from shrinking cells in the outer cortex diffuse through the apoplast to plasmodesmata-rich cells of the inner cortex, collenchyma, and phloem; and that solutes cross the barrier by moving through plasmodesmata.

Paired leaflets of *Samanea saman* and related nyctinastic (night-closing) plants spread their laminae apart and toward the sun (open) during daylight, and fold together in sleep movements (close) at night (24). More than 250 years ago, de Mairan (5) reported that leaf movements in the sensitive plant, *Mimosa pudica*, persist in the absence of environmental perturbations. He thus provided the first experimental evidence for endogenous circadian oscillators, commonly called biological clocks. Circadian rhythms have now been documented in algae, fungi, higher plants, and animals, and appear to be a fundamental feature of eukaryotic organization. In many organisms, they are part of the photoperiodic time measurement system which assures the appropriate annual timing of certain developmental processes, including reproduction (2).

*Samanea* leaflet movements are entrained by environmental light-dark cycles (24), and are therefore useful for investigating light-clock interactions. The movements are a consequence of

massive fluxes of K, Cl, and other solutes into and out of cells in different regions of the pulvinus (the motor organ at the base of each lamina) (3, 32–34). The ion fluxes display rhythmic and light-mediated sensitivity to metabolic inhibitors, low temperature, and compounds that interfere with the transport of certain ions (reviewed in references 30 and 31), and thus have contributed toward models for light- and clock-driven changes in membrane pumps and channels (31).

Each *Samanea* pulvinus is a highly differentiated structure containing hundreds of thousands of cells. Leaf movements are therefore advantageous for studying rhythmic organization in a multicellular system. Cells in the outer layers of the pulvinus alternately swell and shrink, providing the physical basis for leaf movements. Although cells in the central vascular core undergo little deformation, their excision prevents leaf movements (25). In the research reported here, we identified cells with walls that form barriers to the diffusion of solutes from

shrinking to swelling cells, thereby locating cells and cellular structures with key regulatory roles in leaf movements.

Solutes can move from one plant cell to another either through the symplast (the cytoplasmic continuum, consisting of the cytoplasm and intercellular cytoplasmic bridges, called plasmodesmata) or through the apoplast (cell walls and intercellular spaces). Solutes that follow the apoplastic pathway must cross the plasmalemma of the cell losing solute, then diffuse through the apoplast and cross the plasmalemma of the cell taking up solute. The symplast is the only available pathway if hydrophobic barriers block diffusion through the apoplast.

Earlier analyses of K and Cl distribution in thick (~40  $\mu\text{m}$ ) freeze-dried sections from open and closed pulvini (reviewed in reference 30) lacked the resolution to differentiate intracellular from extracellular compartments. Recently, we developed methods which permit this differentiation (3). These techniques involve cutting and dehydrating thin (~100 nm) cryosections of unfixed, uncryoprotected, quench-frozen pulvinar tissue which are then analyzed with a scanning electron microscope (SEM) equipped with an energy-dispersive x-ray analyzer. Using these methods, we found that the apoplast is an important pathway for solute redistribution in the pulvinus, while plasmalemma membranes are important control barriers (3). However, these same studies revealed high K and Cl in the flexor<sup>1</sup> apoplast and low K and Cl in the extensor<sup>1</sup> apoplast of closed pulvini, raising questions about how this ion gradient is maintained. By further SEM/x-ray microanalysis of freeze-dried thin sections, we have obtained evidence for hydrophobic barriers between extensor and flexor, implying that symplastic transport is also necessary for redistribution of ions.

## MATERIALS AND METHODS

### Plant Material and Growing Conditions

*Samanea saman* (Jacq.) Merrill plants were grown at  $27^\circ \pm 1^\circ\text{C}$  in a controlled environment chamber with 16-h light:8-h dark cycles ( $180 \mu\text{mol m}^{-2} \text{s}^{-1}$ , supplied by Sylvania Cool White fluorescent tubes). Terminal secondary pulvini (32) from the third through ninth fully developed leaves (counting from the apex) were used for all experiments. Except where noted, pulvini were excised under dim green light between hours 1 and 3 of the dark period, when leaflets were completely closed; pulvini for Fig. 5 and Table II were excised in white light between hours 1 and 3 of the photoperiod, when leaflets were completely open.

### Evaluation of Different Cryotechniques Applied to Plant Tissue

In preparing biological material for SEM/x-ray microanalysis of diffusible elements, rapid freezing of the tissue minimizes the displacement of solutes and the formation of ice crystals (1). A number of cryological techniques have been developed for tissue preparation, but most are only suitable for particular tissue types or for specific kinds of analyses. For example, freeze substitution techniques have been applied to plant tissues by several investigators (14, reviewed in 20). Freeze substitution can provide adequate structural preservation, but preventing displacement of highly diffusible ions during replacement of tissue  $\text{H}_2\text{O}$  by organic solvents is a major problem (20). Analysis of fractured frozen bulk specimens in an SEM equipped with a cold stage (8, 26) is another useful technique. This method has the advantage of permitting analysis of solutes in the vacuoles. However, the optimal spatial resolution for potassium has been estimated as 2.0–2.5  $\mu\text{m}$  (13, 26). Since the walls of many cortical cells in the *Samanea* pulvinus are thinner than this (21), the method is not suitable for localizing elements in the *Samanea* apoplast.

<sup>1</sup> The pulvinus is divided longitudinally into two functional halves (see Fig. 6); cells in the *extensor* half swell during leaflet opening and shrink during closure; cells in the *flexor* half behave in the opposite manner (32). The extensor-flexor axis is displaced by approximately  $45^\circ$  from the dorsal-ventral axis.

To obtain improved spatial resolution together with minimum displacement of diffusible elements, we developed methods for preparing thin freeze-dried cryosections without use of chemical fixatives or cryoprotectants (3). Similar methods have been widely used for the subcellular localization of elements in animal tissues (1, 38, reviewed in 37), but to our knowledge had not previously been applied to tissues of higher plants. Using these methods, we can clearly and consistently differentiate elements in the walls from those in the cell interior, as demonstrated below (Fig. 5). However, the tonoplast disrupts during tissue preparation and elements in the vacuole mix with elements in the cytoplasm. Consequently, we refer to the interior of the cell simply as the "protoplast."

### Preparation of Cryosections

We selected small secondary pulvini (~1.0–1.5 mm diameter) from healthy *Samanea* plants and excised a single cylindrical segment (~1 mm long) from each pulvinus. To facilitate cutting cryosections, we trimmed each pulvinar segment with a razor blade, making two parallel longitudinal cuts. The two cuts removed a few cell layers from the outer cortex of the flexor and extensor regions, and were roughly parallel to the plane dividing extensor from flexor.

The trimmed pulvinus was mounted on the head of a silver pin (LKB 94-92-0592) using a drop of glycol/resin embedding medium (Tissue Tek, American Scientific Products, McGaw Park, IL) to secure the base of the tissue to the pin. The pin, mounted in a spring-loaded "gun" (LKB 90-00-2395), was injected into Freon 22 that had been supercooled by a liquid nitrogen bath to  $-155^\circ\text{C}$  (measured at the depth to which specimens were injected). The freezing vessel was filled completely with Freon 22 to minimize formation of a layer of cold gas above the liquid, and the Freon 22 was stirred constantly to avoid the formation of temperature gradients (9). The entire process, from excision to freezing, was <30 s. Frozen samples were stored in liquid nitrogen for up to 1 wk, until they were sectioned.

The frozen tissue was sectioned with a diamond knife maintained at  $-70^\circ\text{C}$  in an LKB Ultratome V equipped with an insulated chamber maintained at  $-75^\circ\text{C}$ . Section thickness, controlled by a setting on the microtome, was nominally 100 nm. The first several sections from each block were discarded, until complete transverse sections of the pulvinus were obtained. This was necessary to compare elements in the apoplast of cells from different regions of the pulvinus. Some structural preservation was probably sacrificed, since other investigators (38, reviewed in 37) have detected ice crystals in sections further than 10–20  $\mu\text{m}$  from the surface of the tissue exposed during freezing. Ice crystals in plant cells are most evident in the vacuoles (26); this might account for disruption of tonoplast membranes in our sections.

Successive sections formed a ribbon that was teased flat with a chilled eyelash probe and collected on a chilled Formvar-coated slot grid. Although formation of a ribbon implies that parallel edges of the section melt to adhere to one another, Appleton (1) was unable to detect ion redistribution during this process. The grids were placed on a chilled polished carbon planchet (E. F. Fullman, Schenectady, NY) and covered by a second planchet. A 100-g weight was placed on top of the sandwich to flatten the sections. Sections were transferred to a chilled glass desiccator and dehydrated over phosphorus pentoxide ( $\text{P}_2\text{O}_5$ ) as previously described (3), except that dehydration was more gradual ( $-75^\circ\text{C}$  for 1–2 h,  $-60^\circ\text{C}$  overnight,  $-18^\circ\text{C}$  for 3–4 h,  $3^\circ\text{C}$  for 3–4 h, room temperature until equilibration). Dried sections were stored on carbon planchets over dry  $\text{P}_2\text{O}_5$  in a desiccator at atmospheric pressure until analyzed. Under these storage conditions, ion distribution patterns remained stable during several months of storage, as demonstrated by the reproducibility of results from sections cut at the same time but analyzed months apart. Sections were inserted into the SEM only once, to obviate the possibility that water-soluble ions might redistribute during the transfer from vacuum to atmospheric pressure.

### X-ray Microanalysis

Sections were analyzed with a Coates-Welter SEM equipped with a Tracor Northern 3208-B-VS energy-dispersive x-ray analyzer, interfaced to a Tracor Northern 2000 minicomputer. The operating voltage was 15 kV, beam current was 1–2 nA, counting time was 60 s per probe, and dead time was <20%. The instrument was operated in the spot mode, with a beam diameter of ~2 nm. The x-ray detector was positioned 10 cm from the specimen stage, which was tilted  $45^\circ$ . The x-ray take-off angle was  $25^\circ$ – $27^\circ$  for a flat specimen.

Results are presented both numerically and as energy spectra. Spectral peaks for Cl, K, magnesium (Mg), phosphorus (P), calcium (Ca), and copper (Cu) were identified by the  $K_\alpha$  lines of these elements; the Cu peak at the left end of all spectra is from the copper slot grid with which sections were collected; other peaks are from elements in the plant tissue. The x-ray analyzer is also sensitive to sodium (Na), but the pulvinus contains very little of it (32), and a statistically significant Na peak was not observed in any of our tissue. Information from spectra was quantified by a best-fit computer program which matched spectra from our sections to spectra obtained from crystallized  $\text{MgCl}_2$ ,  $\text{NaH}_2\text{PO}_4$ , KCl,

and  $\text{CaCl}_2$  standards. This program (described in reference 35) aids in deconvoluting peaks from adjacent elements on the periodic table (e.g. K and Ca); deconvolution is required because the  $K_{\beta}$  peak of the lighter element sometimes overlaps the  $K_{\alpha}$  peak of the adjacent heavier element. Tabular data represent peak values (scintillations in the element's spectral window after subtraction of background scintillations), divided by background scintillation counts at 4.6–5.1 keV (a region lacking elemental peaks). This peak/background ratio is more reliable than the peak value alone, as discussed by Roomans (29). Peak values were corrected for contamination using spectra collected from regions of the Formvar membrane on which the sections were mounted, but several micrometers distant from the tissue. We detected low levels of Cl contamination (peak/background ratios of  $\sim 0.1$ ) in some samples. Markhart and Lauchli (19) also reported Cl contamination in outer regions of samples quenched in Freon 22, whereas samples quenched in liquid nitrogen or a liquid nitrogen slush were free of Cl contamination. However, both liquid and slushy nitrogen are markedly inferior to Freon 22 in their cooling rates (4, 9), and *Samanea* tissue frozen in nitrogen sectioned poorly.

Only those spectra obtained in a single day are compared, because operating conditions varied from one day to another. Peak/background ratios for K and Ca were multiplied by 3.15 and 2.40, respectively, to correct for the less efficient detection of these elements compared to Mg, P, and Cl. These correction factors are based on measurements of the crystallized standards described above.

We selected sections (or areas within sections) with adequate morphological preservation for x-ray microanalysis. We rejected structures that could not be identified unambiguously as apoplast or protoplast and parts of the tissue that were thin and shredded or highly charged in the SEM. Nevertheless, certain difficulties are inherent, given the physical properties of the *Samanea* pulvinus. For example, the density of the protoplast in both extensor and flexor cells varies rhythmically, with rhythms in these two cell types  $\sim 180^\circ$  out of phase with one another (32). Thus, cryosectioning at a constant thickness cannot be expected to produce sections of absolutely uniform thickness, particularly after dehydration. Uneven specimen topography, resulting from differences in the density of the cell wall compared to the protoplast, is another factor whose impact on x-ray microanalysis is difficult to assess. Consequently, our numerical data must be

regarded as semi-quantitative, a conclusion also reached by others reviewing the present state of SEM/x-ray microanalysis (15, 29, 37).

## Microscopy

Freeze-dried sections were sputter-coated with gold after elemental analyses were completed, and photographed in the SEM. Tissue for light and transmission electron microscopy was fixed in cold 2% glutaraldehyde-2% paraformaldehyde in 100 mM Na phosphate buffer (pH 7.1), postfixed in cold 1% osmium tetroxide, dehydrated in an ethanol series, and infiltrated slowly (1 wk) in epoxy resin (Epi Rez 5071, R. H. Carlson Co., Greenwich, CT). 1.0- $\mu\text{m}$  thick sections were stained with toluidine blue for light microscopy; 70-nm thick sections were stained with lead citrate for transmission electron microscopy.

Fresh tissue for light microscopy was sectioned ( $\sim 25 \mu\text{m}$ ) with a vibrating microtome (Vibratome, Series 1000, Ted Pella Inc., Irvine, CA) and stained with Sudan B black or Sudan IV to reveal hydrophobic regions of cell walls (16). The sections were examined with a light microscope; because they were relatively thick and photographed poorly, information was reproduced by free-hand drawings.

## RESULTS

### Structure of Freeze-Dried and Fixed Tissue

Preparation of thin freeze-dried cryosections of biological tissue without use of chemical fixatives or cryoprotectants is a relatively new technique. Plant tissue presents special problems, since plant cell contents are frequently thin bands of cytoplasm surrounding large liquid-filled vacuoles. Cell walls may be tough or hardened, and difficult to thin section in the absence of a polymerized matrix. It was therefore important to examine cell and tissue structure in chemically fixed as well as freeze-

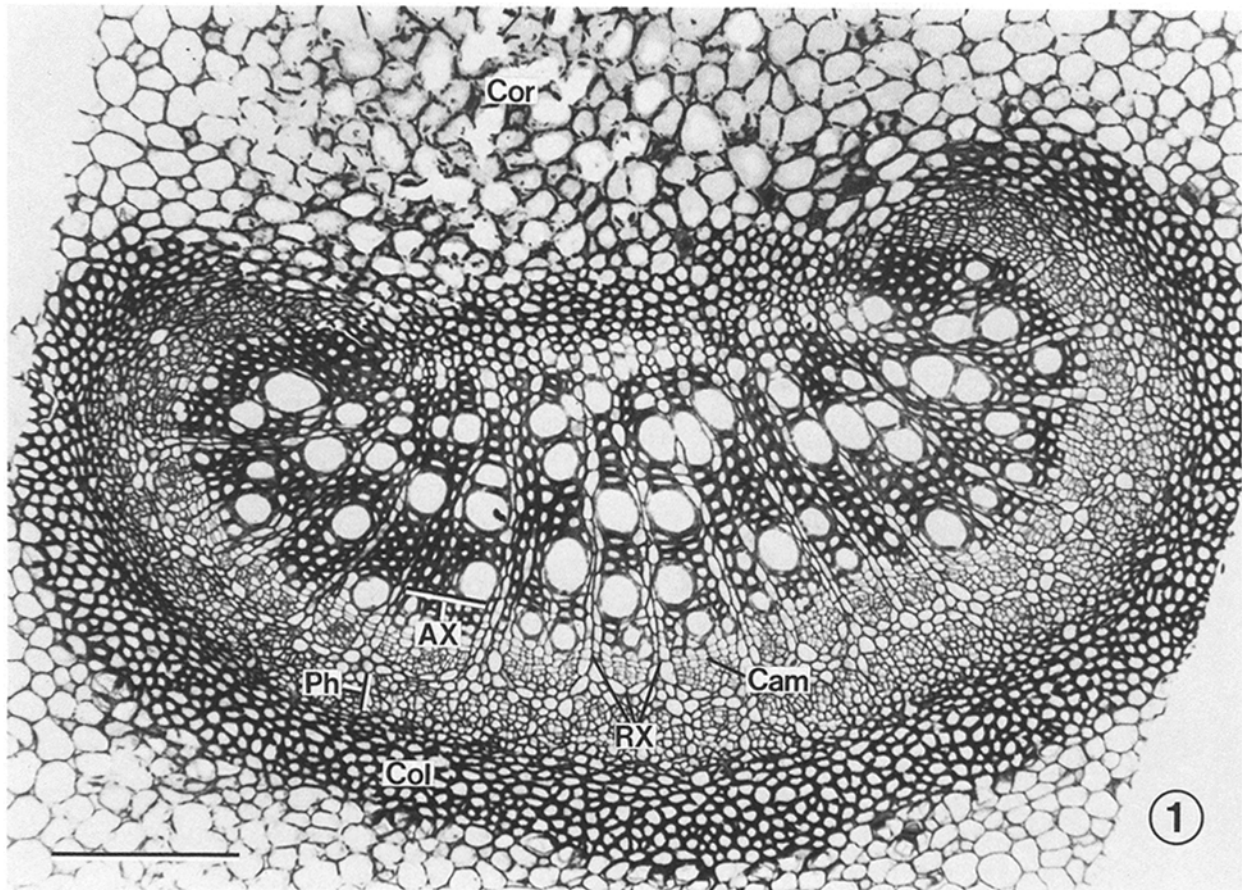


FIGURE 1 Light micrograph of chemically fixed, toluidine blue stained pulvinar tissue, showing the central vascular core in transverse section. The tissue is composed of axial xylem (AX); ray xylem (RX); vascular cambium (Cam); phloem (Ph); collenchyma (Col); and cortex (Cor). Bar, 0.5 mm.  $\times 50$ .

dried cryosections, although elemental analyses were performed only on cryosections.

The pulvinus is a flexible cylinder, straight when leaflets are open and curved when they are closed (32). Its kidney-shaped central vascular core (Fig. 1) is surrounded by 20–30 layers of cortical cells (21; micrograph in 3). The vascular tissue is composed of xylem bordered by several layers of phloem, in turn bordered by several layers of collenchyma-like cells (in all but the concave region of the vascular core [Fig. 1]). The thick walls of the collenchyma cells function as a reservoir for the storage of K, Cl, and other solutes (3).

The xylem consists of axial tissue interspersed by rays (Fig. 1). These structures are preserved sufficiently well in freeze-dried cryosections (Fig. 2) to enable elements in axial xylem to be distinguished readily from those in ray tissue. Cells in the phloem and collenchyma contain large pit fields (Fig. 3 *a*) with numerous plasmodesmata (Fig. 3 *b*), as also described for *Mimosa* pulvini (11).

Cells in the innermost layer of the cortex contain large Ca crystals (Fig. 4 *a*), as identified by their x-ray spectra (Fig. 4 *b*). In cryosections, Ca is the only element with a peak in the crystal's x-ray spectrum, yet Ca is barely detectable in the walls of the same cell (Fig. 4 *c*), indicating that it has not been redistributed from crystal to wall during cryosectioning or freeze-drying. Similarly, probes made in the vacuole 0.5  $\mu\text{m}$  from the crystal yielded Ca values <1.5% of those in the crystal,

whether the regions probed were north, south, east, or west of the crystal.

Fig. 5 *a* shows a cell in the flexor outer cortex of a white-light opened pulvinus, as seen in freeze-dried sections. The protoplast, cutinized outer epidermal walls, and interior walls can be readily differentiated. The integrity of these structures is apparently preserved during cryosectioning and freeze-drying, since the amount of K, Cl, and other elements differ for outer compared to interior walls, and for the wall compared to the protoplast (Figs. 5 *b–d*). Tonoplast membranes, by contrast, are apparently disrupted during tissue preparation, as discussed above. We were thus unable to distinguish vacuolar from cytoplasmic compartments (3).

### Elemental Analysis

We analyzed elements in compartments designated as (*a*) apoplast or wall, and (*b*) protoplast. The former contains solutes from cell walls and contiguous water-filled intercellular spaces; the latter contains solutes from vacuoles and cytoplasm. Our goal was to localize barriers to the diffusion of solutes through the apoplast. We reasoned that a sharp discontinuity in the solute content of walls of adjacent cells (or different walls of the same cell), if consistently observed, would provide evidence for such a barrier. We previously analyzed K and Cl in the apoplast surrounding cortex and collenchyma cells located in the middle of the extensor and flexor regions, and

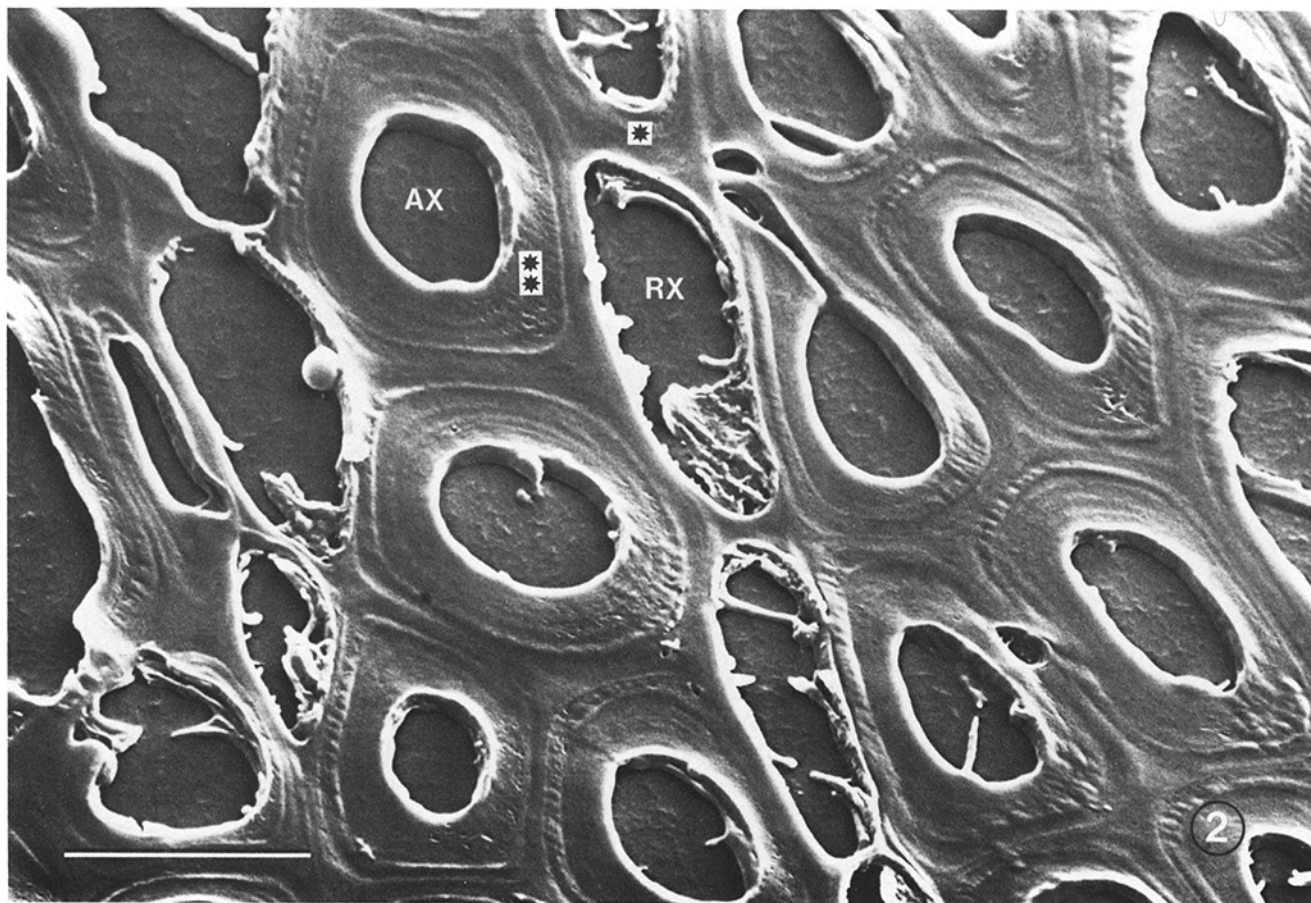


FIGURE 2 Scanning electron micrograph of freeze-dried, cryosectioned tissue showing cells of the axial and ray xylem. Axial xylem cells are water-conducting tracheary elements, which are nonliving and devoid of protoplasts at maturity. Elements were analyzed in the end (tangential) wall of a ray cell (\*) and in the wall between axial and ray tissue (\*\*); resulting x-ray data are in Table I. Bar, 5  $\mu\text{m}$   $\times$  6,500.

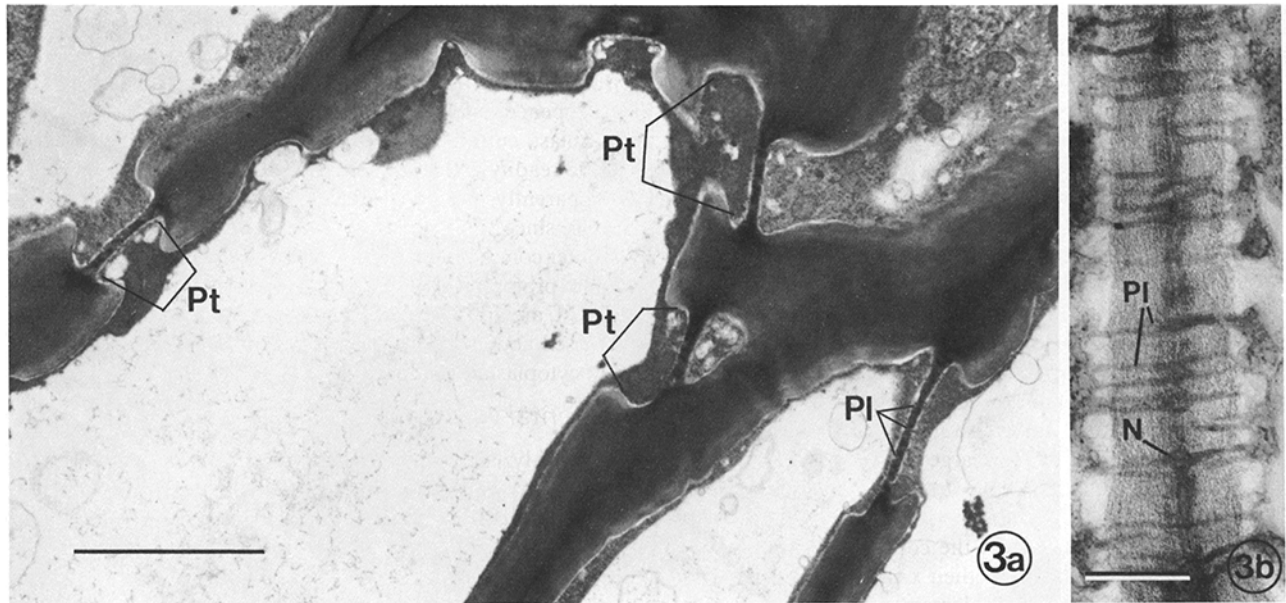


FIGURE 3 Transmission electron micrographs of chemically fixed tissue, showing collenchyma cells in longitudinal section. (a) Large pit fields (*Pt*) in cell walls, containing numerous plasmodesmata (*Pl*). Bar, 5  $\mu\text{m}$ .  $\times$  5,100. (b) A pit field at higher magnification. Note the many plasmodesmata. Median nodules (*N*) are apparent in several of the plasmodesmata. Bar, 0.5  $\mu\text{m}$ .  $\times$  28,000.

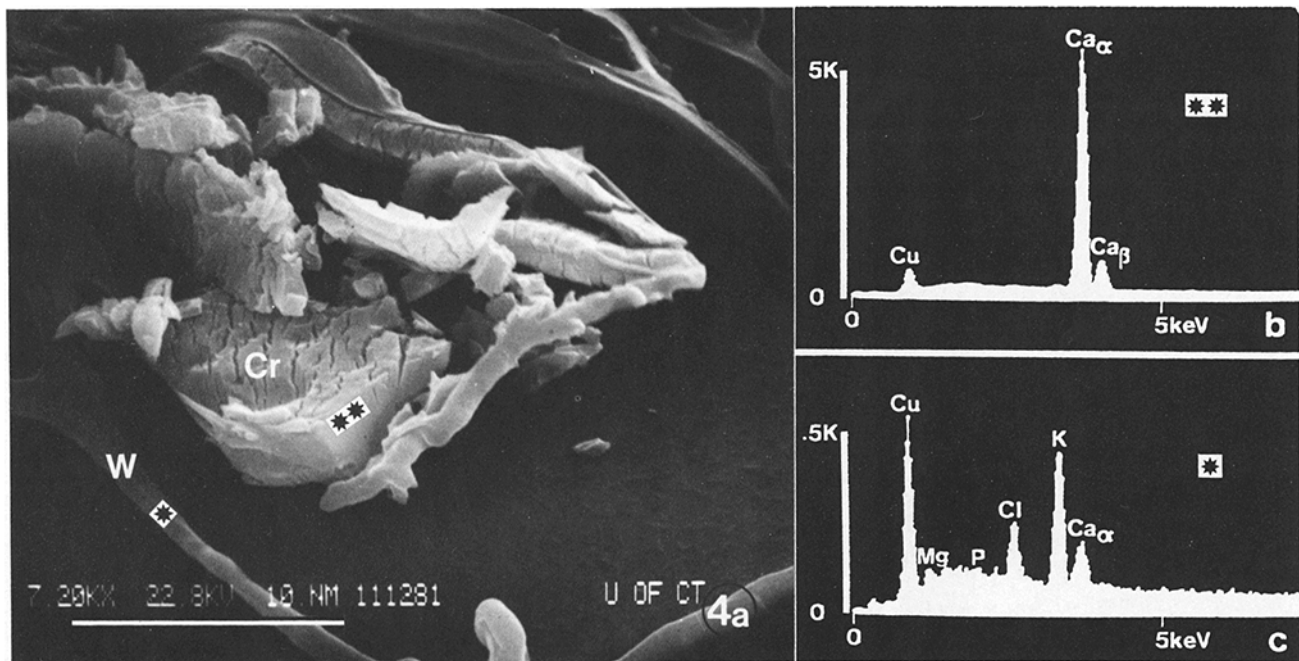


FIGURE 4 Freeze-dried cryosection of pulvinal tissue, showing a cell from the inner cortex with a Ca crystal. (a) Scanning electron micrograph. Crystal (*Cr*); cell wall (*W*). Bar, 5  $\mu\text{m}$ .  $\times$  7,200. (b) Energy spectrum of elements in the crystal; probe made at (\*\*) in (a). (c) Energy spectrum of elements in the wall; probe made at (\*) in (a).

found that extensor-flexor differences were most pronounced when leaflets were closed (3). We therefore used pulvini from closed leaflets for all of our analyses, except those presented in Table II.

Initially, we probed the walls surrounding cells in the outer cortex at mid-flexor and mid-extensor (\*\* in Fig. 6); K in the former was  $\sim$ 20 times greater than K in the latter, confirming previous results (3). Chloride distribution was similar to that of K, but absolute values (scintillations/60 s) were only 15–20% those of K, after correcting for differences in detection efficiency as described above. We then analyzed the walls of

contiguous cortical cells, starting at mid-flexor and moving the probe circumferentially, both clockwise and counterclockwise. K and Cl were consistently high until cells halfway between mid-flexor and mid-extensor were probed. Potassium and Cl (and also Ca and Mg) were high in one radial wall of these cells (the wall closest to mid-flexor), very low in tangential walls, and virtually absent from the other radial wall and all walls of subsequent cells in the extensor direction (Fig. 7).

Cells along radii extending from the epidermis to the inner edge of the phloem on both upper and lower sides of the tissue showed similar properties: a one-wall-wide discontinuity be-

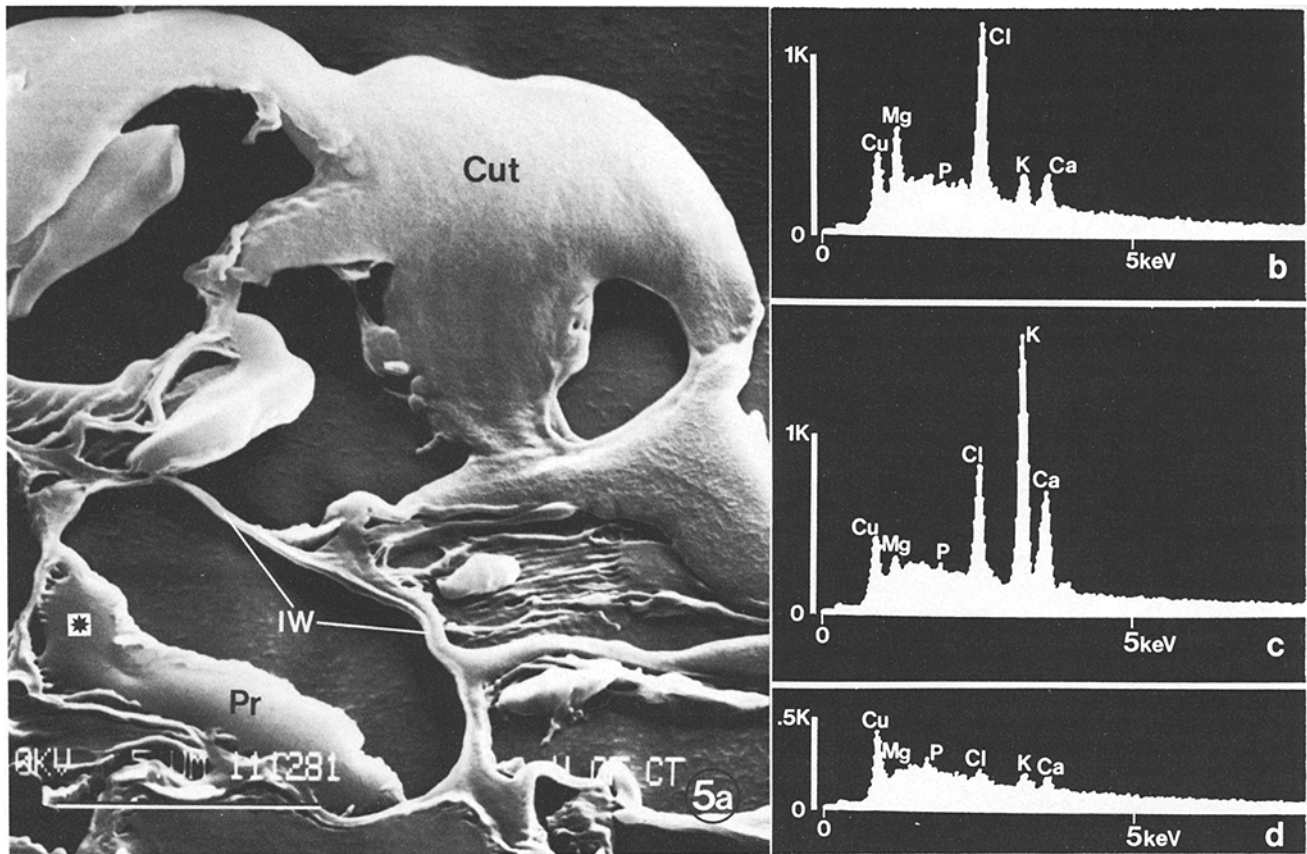


FIGURE 5 Freeze-dried cryosection of pulvinar tissue, showing cells in the outer cortex of the flexor region of a pulvinus that opened in white light. (a) Scanning electron micrograph. Cuticle layer of outer epidermal cell (*Cut*); interior wall (*IW*); protoplast (*Pr*). Bar, 5 μm. × 7,000. (b) Energy spectrum of elements in the protoplast; probe made at (\*) in (a). (c) Energy spectrum of elements in the inner tangential wall of an epidermal cell. (d) Energy spectrum of elements in the outer tangential wall of an epidermal cell.

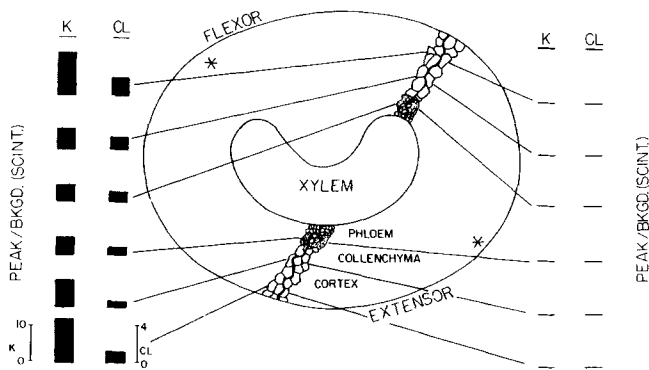


FIGURE 6 Schematic drawing of a transverse section through the pulvinus, emphasizing cells at the interface of the extensor and flexor. The heavy lines extending from the epidermis to the xylem represent cell walls with high K and Cl levels; the protoplast and walls of all cells to the left of the line also have high K and Cl; those to the right of the line are virtually devoid of both ions. The bar graphs give average corrected K and Cl values (scintillations [peak]/scintillations [bkgd.]) for the walls of cells in six regions on each side of the division. Mid-extensor and mid-flexor regions are indicated by (\*).

tween a region of the apoplast rich in K and other elements, and a region devoid of these elements. This sharp discontinuity in the solute content of the apoplast could be explained by a barrier to ion diffusion functionally similar to the Casparian strip that surrounds the stele in plant roots (10).

Cortical cells on the "high K" side of the barrier in the

pulvinus also had high internal K, while cortical cells on the other side of the barrier had very little internal K (Fig. 7). When pulvini are closed, cells with high internal K are called flexor cells, while cells with low internal K are called extensor cells, according to previous definitions of these terms (32). Thus the apoplastic barrier was at the interface of the extensor and flexor regions.

If the barrier provides a complete functional separation between extensor and flexor, it must either traverse or surround the xylem. The first possibility predicts a discontinuity in apoplastic solutes in different regions of the xylem, while the second predicts a discontinuity in apoplastic solutes between the xylem and the surrounding phloem. As Table I indicates, K did not vary significantly for different regions of the apoplast within axial xylem, including walls between axial and ray xylem, but these walls had only 40% as much K as did the end (tangential) walls of ray xylem cells (Fig. 2). It therefore appears that the walls separating axial from ray cells form a barrier to the free diffusion of solutes between these two cell types. However, we did not determine whether the barrier was in the wall of the ray cell, the axial xylem cell, or both.

The apoplast of axial xylem also had less K than that of the phloem and collenchyma (Table I). The division between low and high K lay between xylem and phloem, with the cambium (a single or double row of meristematic cells that give rise to secondary xylem and phloem) on the low K side of the barrier. Thus barriers in and around the cambium, in combination with the barrier penetrating the phloem, collenchyma, and cortex (Fig. 6), completely separated extensor and flexor apoplasts.

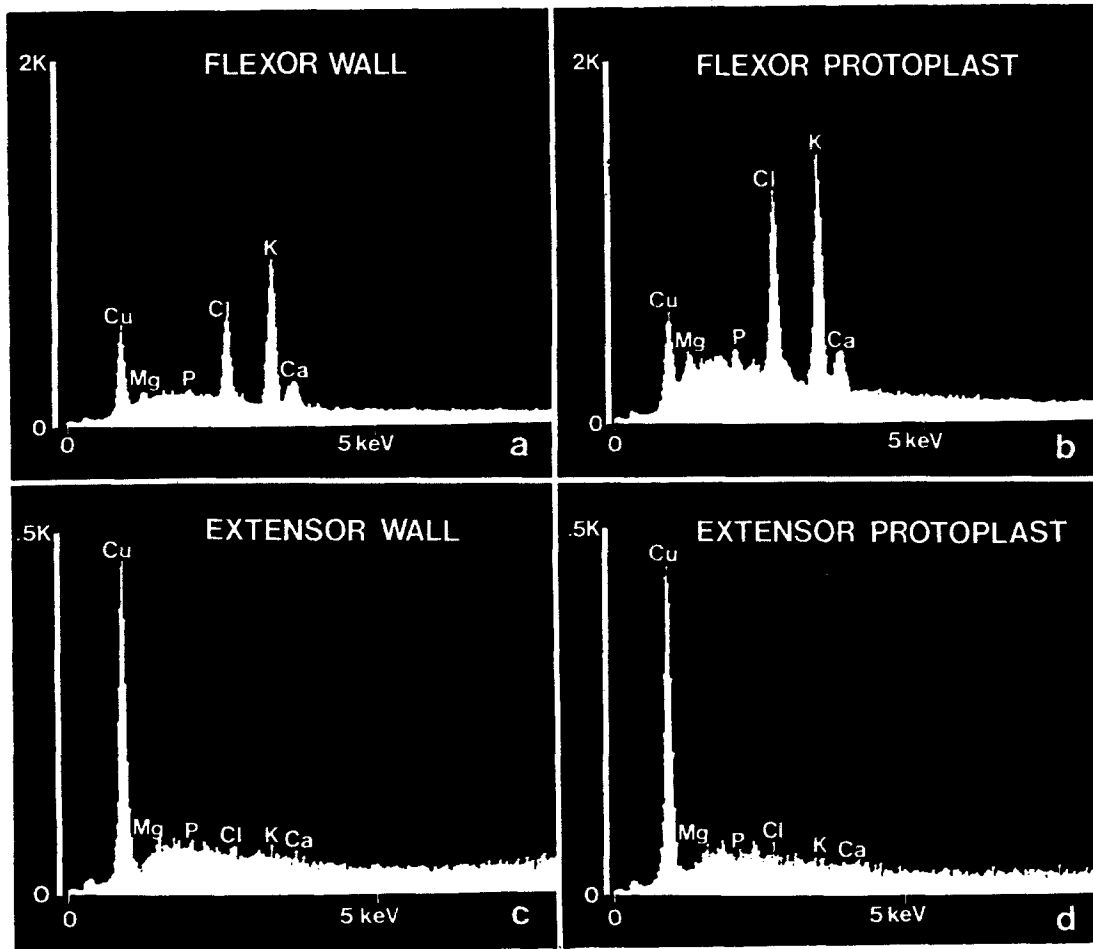


FIGURE 7 Energy spectra of walls (a, c) and of protoplasts (b, d) from typical cells on the flexor and extensor sides of the extensor-flexor interface. Both cells are in the mid-cortex, on the upper side of the pulvinus. Spectra of flexor wall and protoplast reveal small Mg, P, and Ca peaks as well as large Cl and K peaks.

TABLE I  
Elements in the Walls of Vascular Tissue of *Samanea pulvini*

Region probed	n*	Na	Mg	P	Cl	K	Ca*
Ray xylem, tangential wall‡	3	0.00 ± 0.00§	0.00 ± 0.00	0.02 ± 0.01	0.19 ± 0.01	2.71 ± 0.12	0.24 ± 0.05
Axial xylem‡	6	0.00 ± 0.00	0.01 ± 0.01	0.05 ± 0.02	0.19 ± 0.01	1.03 ± 0.05	0.06 ± 0.01
Phloem	10	0.00 ± 0.00	0.10 ± 0.08	0.08 ± 0.01	0.38 ± 0.02	2.82 ± 0.11	0.43 ± 0.05
Collenchyma	6	0.00 ± 0.00	0.06 ± 0.02	0.03 ± 0.00	0.44 ± 0.02	2.57 ± 0.17	0.32 ± 0.09

\* Number of observations, each from a different cell. Data were pooled from two sections. Both sections were in the flexor region of a closed pulvinus.

‡ See Fig. 2 for regions probed.

§ Corrected peak:background ratios, as described in text. Data presented as mean ± SE. Ratios of .00 were recorded when no peak was detectable above background levels.

We then compared elements in exterior and interior walls of epidermal cells (Table II). Since exterior epidermal walls are usually impregnated with cutin and other hydrophobic compounds, one would expect these walls to form an additional barrier to solute diffusion. Elemental analysis confirms this prediction; solutes in outer walls are only 10–20% those in interior walls.

#### Use of Sudan Stains to Localize Hydrophobic Walls

To test further for barriers to solute diffusion through the apoplast, we stained 25- $\mu$ m thick sections of fresh tissue with

Sudan B black and Sudan IV, two lipid-soluble dyes used to identify hydrophobic cell walls (16). Both dyes give colored reactions in the presence of lipids (deep blue to black with Sudan B black, and pink with Sudan IV). When the tissue was soaked in Sudan B black, outer epidermal walls stained deep blue, while walls surrounding xylem rays and walls separating cambium from phloem, both stained black. Epidermal walls characteristically contain cutin, while hydrophobic interior walls characteristically contain suberin (18). Cells whose walls absorb Sudan B black are shown diagrammatically in Fig. 8 (see figure legend for additional details). These cells also stained pink when soaked in Sudan IV. However, neither dye gave a color reaction along the extensor-flexor division iden-

TABLE II  
Elements in the Walls of Epidermal and Sub-Epidermal Cells of *Samanea Pulvini*

Region probed	n*	Na	Mg	P	Cl	K	Ca
Outer wall of epidermal cell	3	0.00 ± 0.00†	0.13 ± 0.07	0.05 ± 0.02	0.20 ± 0.17	0.95 ± 0.25	0.47 ± 0.09
Interior wall§	8	0.00 ± 0.00	0.49 ± 0.04	0.33 ± 0.10	2.16 ± 0.16	11.19 ± 1.27	4.44 ± 0.33

\* Number of observations, each from a different cell in the same section. Data are from the flexor region of an open pulvinus.

† Corrected peak:background ratios, as described in text. Data presented as mean ± SE. Ratios of 0.00 were recorded when no peak was detectable above background levels.

§ Epidermal and subepidermal cells.

tified in Fig. 6, indicating that this barrier either differs chemically from barriers in the epidermis and vascular tissue or is too thin to be resolved by this technique.

## DISCUSSION

### Apoplastic Barrier Separating Extensor from Flexor Regions

Several years ago, we reported large discontinuities in K and Cl at the extensor-flexor interface of closed *Samanea pulvini* (34). Since the detection method lacked the resolution to discriminate between intracellular and extracellular elements, it seemed possible that the discontinuities were solely in protoplasmic solutes, explicable by rhythmic pumps and/or channels that peaked at different times in extensor and flexor cells. This postulate must now be modified, for we have demonstrated that apoplastic as well as protoplasmic solutes are discontinuous at the extensor-flexor border. As our working hypothesis, we propose that extensor-flexor differences in solute content arise in part by differentially phased, plasma-membrane-localized pumps and channels (see supporting data in reference 3), and in part by barriers to the free diffusion of water-soluble substances through the apoplast (Fig. 9). The nature of the barrier at the extensor-flexor interface remains to be determined. Since these cells fail to stain after treatment with Sudan dyes, the barrier probably differs chemically from barriers surrounding the cambium and ray xylem, and from cutin-impregnated outer epidermal walls.

Our evidence for an apoplastic extensor-flexor barrier is based on elemental analysis of only closed pulvini, but it is likely that the barrier is fixed and present at all parts of the rhythmic cycle. Reexamination of earlier data (see Fig. 1 in reference 34) reveal a discontinuity near the extensor-flexor region in all pulvini analyzed (leaflet angles ranged from  $-10^\circ$  to  $110^\circ$ ), although the older detection method lacked the resolution to localize the discontinuity with great precision.

It will also be important to identify solutes that occupy wall sites on the low K side of the barrier. Cell walls have a high density of fixed negative charges, and can accumulate 300–500 mM monovalent cations or lesser concentrations of polyvalent cations (6, 27). Since Na and heavier elements are detectable in our SEM/x-ray analyzer but were not observed in the extensor apoplast of closed pulvini (Fig. 7), likely candidates are lighter elements such as protons (31) or organic cations such as polyamines (17).

### Movement of Solutes Across the Barrier

Virtually all pulvinar K is on the flexor side of the barrier when leaflets are fully closed. Approximately 60% of these ions migrate to the extensor during opening and back to the flexor 12 h later, when leaflets close again (34). If an apoplastic

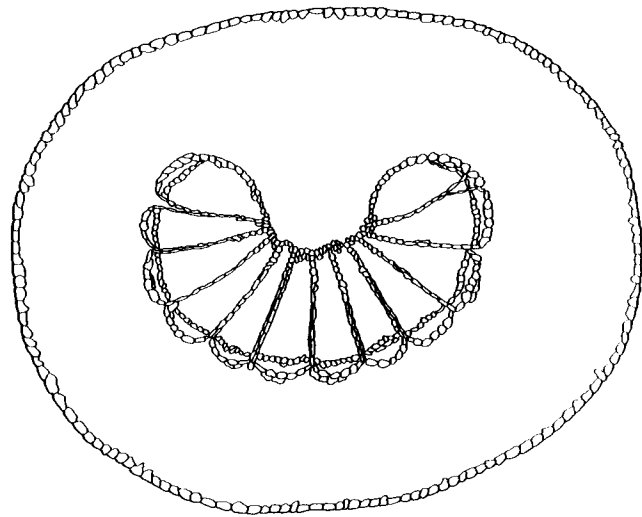


FIGURE 8 Schematic drawing of cells whose walls stain blue or black after treatment with Sudan B black. The color reaction occurs in walls of epidermal cells, and at the interface of axial xylem/ray xylem, phloem/ray xylem, and cambium/phloem. End walls of ray xylem are also shown to clarify cellular morphology, but do not stain. All walls of epidermal cells are also shown, although the method lacked the resolution to determine whether inner as well as outer epidermal walls stain. The method also lacked the resolution to determine whether end walls of cells at the cambium-xylem interface absorb stain.

barrier separates extensor and flexor, solutes must move through the symplast to cross the barrier. There are relatively few plasmodesmata in the outer cortex (Table 1 in reference 21), but plasmodesmata are highly concentrated in the phloem, collenchyma, and one or two innermost cell layers of the cortex of *Samanea* (Fig. 3 and Satter, unpublished data) and *Mimosa* (11) pulvini. It therefore seems likely that solutes from shrinking cells in the outer cortex migrate through the apoplast to the inner cortex, collenchyma, and phloem, where they enter the symplast for passage through the barrier. Note that apoplastic solutes decrease continuously from outer to inner tissues (Fig. 6), as would be expected if solutes diffuse to inner cells to enter the symplast. This hypothesis is also consistent with reports by Pfeffer and other nineteenth-century botanists (25) that pulvinar movements persist after selective dissection of portions of the tissue, but only if the central vascular tissue remains intact.

Since the extensor-flexor barrier penetrates both dorsal and ventral sides of the pulvinus, solutes could conceivably cross the barrier through plasmodesmata on one side of the tissue during opening, and through plasmodesmata on the opposite side during closure. If so, the plasmodesmata would function as unidirectional passageways, leading to K distribution patterns that depend upon the direction of leaflet movement as



well as leaflet angle. Kinetic analyses of K distribution in pulvini of opening and closing leaflets do not support this view (34). Potassium distribution patterns are similar for leaflets with similar angles, whether leaflets are opening or closing.

Alternatively, individual plasmodesmata could function as bidirectional passageways. Ultrastructural studies reveal two distinct channels in the plasmodesma: a desmotubule, possibly derived from endoplasmic reticulum, and a cytoplasmic annulus which lies between the desmotubule and the outer limiting membrane, a projection of the plasmalemma (28). Valve-like structures surrounding the necks at both ends of the plasmodesma (23) have been postulated to regulate symplastic transport by modulating the volume of the cytoplasmic annulus (12), and might aid in promoting net solute migration from extensor to flexor during closure, and vice-versa during opening. We are investigating the ultrastructure of plasmodesmata from open and closed pulvini to determine whether structural modifications are associated with leaflet movements.

We have drawn a model (Fig. 10) for solute transfer between cells of the outer cortex on opposite sides of the pulvinus. This modifies and updates an earlier model (31) that was constructed before evidence for an apoplastic barrier in the cortex between extensor and flexor. Our present model proposes that outer cells in either half of the pulvinus lose K and other solutes (presumably due to low pump activity or leaky membranes) while simultaneously, inner cells in the same half-pulvinus accumulate solutes (presumably due to the predominance of pumps over leaks). Solutes then move through the symplast to cross the barrier, although there is controversy as to whether solute movement through plasmodesmata occurs purely by diffusion or requires metabolic energy (12). When *Samanea* leaflets close, the extensor half of the pulvinus is depleted of K and Cl ions (Fig. 6), indicating that solutes are transferred to the flexor against the concentration gradient. It is therefore necessary to postulate that energy is consumed either for transport through plasmodesmata that span the extensor-flexor barrier, or for unloading from symplast to apoplast on the flexor side of the barrier.

### Hydrophobic Barriers Surrounding Axial and Ray Xylem

The xylem provides another possible route between extensor and flexor, involving solute migration through the symplast to cross hydrophobic barriers separating phloem from cambium or ray xylem. However, if solutes traversed axial xylem, they would be swept upward in the transpiration stream; this is incompatible with evidence that very little K is lost from the pulvinus during an oscillatory cycle (36). The xylem rays constitute another possible pathway, but represent only a small fraction of the xylem volume. Furthermore, not all rays extend from flexor to extensor. It therefore seems unlikely that the xylem is an important pathway for shuttling of solutes from one side of the pulvinus to the other.

### Implications for Rhythmicity in the Pulvinus

Our data suggest that solute movements in the *Samanea* pulvinus are regulated by differentially phased rhythmic pumps and/or channels in outer and inner cells of the extensor region, each 180° out of phase with rhythmic pumps and channels in comparable regions of the flexor, while solute transfer between extensor and flexor is dependent upon plasmodesmata that span the barrier separating these two regions. We postulate

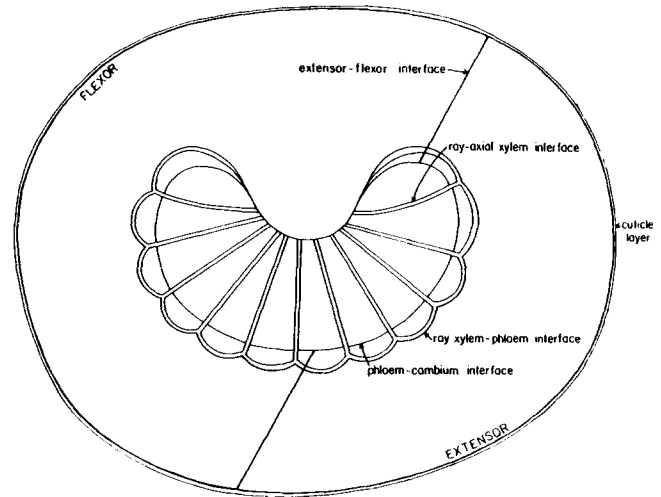


FIGURE 9 A model for barriers to ion diffusion through the apoplast of the pulvinus. The lines represent barriers, based on data in Figs. 6-8 and Tables I and II.

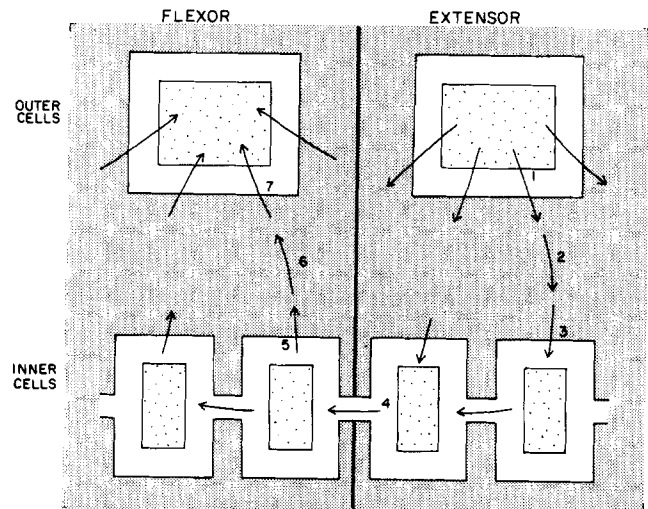


FIGURE 10 A model for combined apoplastic and symplastic transport of K and Cl in the pulvinus during leaflet closure: (1) Efflux across the tonoplast and plasmalemma of extensor motor cells, to the apoplast. (2) Diffusion through the extensor apoplast. (3) Uptake across the plasmalemma into the symplast.\* (4) Movement through plasmodesmata across the hydrophobic barrier.† (5) Efflux through the plasmalemma into the apoplast.‡ (6) Diffusion through the apoplast. (7) Uptake across plasmalemma and tonoplast of flexor motor cells.\*

\* ATP-dependent steps. ATP is probably required for proton secretion, which energizes K and Cl uptake by a chemiosmotic mechanism (31).

† Step 4 or 5 is also ATP-dependent.

that ion movements through plasmodesmata are rhythmic, with net solute transfer from extensor to flexor during closure and vice-versa during opening. Recent studies with other plants suggest reversible mechanisms for regulating solute transfer through plasmodesmata involving either the formation and degradation of callose deposits in the core (7), or valves that regulate solute movements through the cytoplasmic annulus (23). It will be important to determine whether plasmodesmata in *Samanea* pulvini change rhythmically in synchrony with rhythms in the rate and direction of solute movements through them.

Circadian rhythms in membrane structure and transport have been reported in a wide variety of organisms (2). Since membranes control the flow of metabolites into and out of cells and subcellular compartments, rhythms in membrane function would have profound effects on the biochemistry of cells and tissues. Several investigators have postulated that transmembrane ion gradients affect the activity of membrane-localized ion pumps and the opening of diffusion channels, thereby creating a feedback loop that is part of the mechanism for generating circadian oscillations (22, 39). To ensure that such models be applicable to *Samanea*, the role of plasmodesmata, as well as membranes, must be considered.

We are grateful to Dr. Allen Wachtel for numerous helpful discussions and advice, to Jeffrey Staley for developing computer programs for data analysis, to James Romanow for assistance with x-ray microanalysis, to Dr. A. Mugnaini for use of the Vibratome and to Anne-Lise Dahl for instruction in its use, to Ana Iglesias for helping with data analysis, and to Dr. Holly Gorton and two anonymous reviewers for comments on the manuscript.

Supported by grants to R. L. Satter from the National Science Foundation and the University of Connecticut Research Foundation.

Received for publication 5 March 1982, and in revised form 26 July 1982.

## REFERENCES

1. Appleton, T. C. 1974. A cryostat approach to ultrathin 'dry' frozen sections for electron microscopy: a morphological and x-ray analytical study. *J. Microsc. (Oxf.)* 100:49-74.
2. Bünning, E. 1973. *The Physiological Clock*, 3rd Edition. English Universities Press, London.
3. Campbell, N. A., R. L. Satter, and R. C. Garber. 1981. Apoplastic transport of ions in the motor organ of *Samanea*. *Proc. Natl. Acad. Sci. U. S. A.* 78:2981-2984.
4. Costello, M. J., and J. R. Corless. 1978. The direct measurement of temperature changes within freeze-fracture specimens during rapid quenching in liquid coolants. *J. Microsc. (Oxf.)* 112:17-37.
5. de Mairan, M. 1729. *Observation botanique. Histoire de l'Academie Royale des Sciences Paris*. 35.
6. Demarty, M., A. Ayadi, A. Monnier, C. Morvan, and M. Thellier. 1977. Electrochemical properties of isolated cell walls of *Lemna minor* L. In *Transmembrane Ionic Exchanges in Plants*. M. Thellier, A. Monnier, M. Demarty, and J. Dainty, editors. Centre National de Recherche Scientifique et Université de Rouen, Paris et Rouen. 61-73.
7. Drake, G. A., D. J. Carr, and W. P. Anderson. 1978. Plasmolysis, plasmodesmata, and the electrical coupling of oat coleoptile cells. *J. Exp. Bot.* 29:1205-1214.
8. Echlin, P., C. E. Lai, and T. L. Hayes. 1982. Low temperature x-ray microanalysis of the differentiating vascular tissue in root tips of *Lemna minor* L. *J. Microsc. (Oxf.)* 126:285-306.
9. Elder, H. Y., C. C. Gray, A. G. Jardine, J. N. Chapman, and W. H. Biddlecombe. 1982. Optimum conditions for cryoquenching of small tissue blocks in liquid coolants. *J. Microsc. (Oxf.)* 126:45-61.
10. Esau, K. 1965. *Plant Anatomy*, 2nd edition. Wiley and Sons, New York. 515-517.
11. Fleurat-Lessard, P., and J.-L. Bonnemain. 1978. Structural and ultrastructural characteristics of the vascular apparatus of the sensitive plant (*Mimosa pudica* L.). *Protoplasma* 94:127-143.
12. Gunning, B. E. S. 1976. Introduction to plasmodesmata. In *Intercellular Communication in Plants: Studies on Plasmodesmata*. B. E. S. Gunning and A. W. Robards, editors. Springer-Verlag, Berlin. 1-13.
13. Hall, T. A. 1971. The microprobe assay of chemical elements. In *Physical Techniques in Biological Research*, 2nd edition. G. Oster, editor. Academic Press, Inc., NY. 1A:157-275.
14. Harvey, D. M. R., J. L. Hall, T. J. Flowers, and B. Kent. 1981. Quantitative ion localization within *Suaeda maritima* leaf mesophyll cells. *Planta* 151:555-560.
15. Hess, F. D. 1980. Influence of specimen topography on microanalysis. In *X-ray Microanalysis in Biology*. M. A. Hayat, editor. University Park Press, Baltimore. 241-261.
16. Jensen, W. A. 1962. *Botanical Histochemistry*. W. H. Freeman, San Francisco. 259-265.
17. Kaur-Sawhney, R., H. E. Flores, and A. W. Galston. 1981. Polyamine oxidase in oat leaves: a cell wall-localized enzyme. *Plant Physiol.* 68:494-498.
18. Kolattukudy, P. E. 1981. Structure, biosynthesis, and biodegradation of cutin and suberin. *Annu. Rev. Plant Physiol.* 32:539-567.
19. Markhart, A. H., III, and A. Läuchli. 1982. The comparison of three freezing methods for electron probe x-ray microanalysis of hydrated barley root tissue. *Plant Sci. Lett.* 25:29-36.
20. Morgan, A. J. 1980. Preparation of specimens: changes in chemical integrity. In *X-ray Microanalysis in Biology*. M. A. Hayat, editor. University Park Press, Baltimore. 65-165.
21. Morse, M. J., and R. L. Satter. 1979. Relationships between motor cell ultrastructure and leaf movements in *Samanea saman*. *Plant Physiol.* 46:338-346.
22. Njus, D., F. M. Sulzman, and J. W. Hastings. 1974. Membrane model for the circadian clock. *Nature (Lond.)* 248:116-120.
23. Olesen, P. 1979. The neck constriction in plasmodesmata. Evidence for a peripheral sphincterlike structure revealed by fixation with tannic acid. *Planta* 144:349-358.
24. Palmer, J. H., and G. F. Asprey. 1958. Studies in the nyctinastic movement of the leaf pinnae of *Samanea saman* (Jacq.) Merrill. I. A general description of the effect of light on the nyctinastic rhythm. *Planta* 51:757-769.
25. Pfeffer, W. 1907. *The Physiology of Plants*. Vol. III. Translated by A. J. Ewart. Clarendon Press, Oxford, England.
26. Pitman, M. G., A. Läuchli, and R. Steizer. 1981. Ion distribution in roots of barley seedlings measured by electron probe x-ray microanalysis. *Plant Physiol.* 68:673-679.
27. Raschke, K. 1979. Movements of stomata. In *Encyclopedia of Plant Physiology*. Vol. 7. W. Haupt and M. E. Feinleib, editors. Springer-Verlag, Berlin. 383-441.
28. Robards, A. W. 1976. Plasmodesmata in higher plants. In *Intercellular Communication in Plants: Studies on Plasmodesmata*. B. E. S. Gunning and A. W. Robards, editors. Springer-Verlag, Berlin. 15-58.
29. Roomans, G. M. 1980. Quantitative x-ray microanalysis of thin sections. In *X-ray Microanalysis in Biology*. M. A. Hayat, editor. University Park Press, Baltimore. 401-453.
30. Satter, R. L. 1979. Leaf movements and tendrils curling. In *Encyclopedia of Plant Physiology*. Vol. 7. W. Haupt and M. E. Feinleib, editors. Springer-Verlag, Berlin. 442-484.
31. Satter, R. L., and A. W. Galston. 1981. Mechanisms of control of leaf movements. *Annu. Rev. Plant Physiol.* 32:83-110.
32. Satter, R. L., G. T. Geballe, P. B. Applewhite, and A. W. Galston. 1974. Potassium flux and leaf movement in *Samanea saman*. I. Rhythmic movement. *J. Gen. Physiol.* 64:413-430.
33. Satter, R. L., P. Marinoff, and A. W. Galston. 1970. Phytochrome-controlled nyctinasty in *Albizia julibrissin*. II. Potassium flux as a basis for leaflet movement. *Am. J. Bot.* 57:916-926.
34. Satter, R. L., M. Schrepff, J. Chaudhri, and A. W. Galston. 1977. Phytochrome and circadian clocks in *Samanea*. Rhythmic redistribution of potassium and chloride within the pulvinus during long dark periods. *Plant Physiol.* 59:231-235.
35. Shuman, H., A. V. Somlyo, and A. P. Somlyo. 1976. Quantitative electron probe microanalysis of biological thin sections: methods and validity. *Ultramicroscopy* 1:317-339.
36. Simon, E., R. L. Satter, and A. W. Galston. 1976. Circadian rhythmicity in excised *Samanea pulvini*. I. Sucrose-white light interactions. *Plant Physiol.* 58:417-420.
37. Sjöstrom, M. 1980. The skeletal muscle. In *X-ray Microanalysis in Biology*. M. A. Hayat, editor. University Park Press, Baltimore. 263-306.
38. Somlyo, A. V., H. Shuman, and A. P. Somlyo. 1977. Elemental distribution in striated muscle and the effects of hypertonicity. *J. Cell Biol.* 74:828-857.
39. Sweeney, B. M. 1974. A physiological model for circadian rhythms derived from the *Acetabularia* rhythm paradoxes. *Int. J. Chronobiol.* 2:25-33.